Comparison of BN and AlN Substitution on the Structure and Electronic and Chemical Properties of C_{60} Fullerene

Jayasree Pattanayak, Tapas Kar,* and Steve Scheiner

Department of Chemistry and Biochemistry, Utah State University, Logan, Utah 84322-0300

Received: July 16, 2002; In Final Form: March 5, 2003

A comparative study on BN and AlN substitution patterns in C_{60} fullerene and the chemical and electronic properties of these substitutionally doped heterofullerenes has been carried out using semiempirical (MNDO and PM3) and density functional (B3LYP) theories. Several basis sets, namely, 3-21G, 3-21G*, and 6-31G*, are used. Specific systems considered here are $C_{60-2x}(BN/AlN)_x$ where x varies from 1 to 3. Both similarities and dissimilarities have been noticed in the substitution patterns between BN− and AlN−fullerenes. Some of the rules already established in BN substitution patterns are followed by its AlN counterpart. For example, like BN, AlN units prefer to stay together. However, the prominent "hexagon filling rule" of BN−fullerenes is disobeyed by AlN. Its larger atomic size and the weak nature of the Al−N and Al−C π-interaction may be the reason for such discrepancies. AlN substitution causes much more distortion of total electron density of C_{60} than its BN counterpart, making the fullerene easier to oxidize and reduce. The HOMO−LUMO gap (band gap) strongly depends on the number of substituent units, and the changes are minimal for the BN system in comparison to its compeer. Finally, the possibility of dimer formation of BN− and AlN−fullerenes has been studied.

Introduction

Discovery of fullerenes as stable structures of carbon clusters[1] triggered research interest[2−6] not only on these unique carbon cage systems but also on heterofullerenes. Substitution of carbon atom(s) by foreign atoms such as B and N into fullerene cages has been expected to produce significant changes both in the electronic structure and in the possibility of the new types of materials with novel properties. Such heterofullerenes are expected to have wide applications, such as superconductivity, photoelectronic devices, semiconductors, nanometer electronics, etc. The enhanced chemical reactivity of fullerenes by such doping also opens new synthetic routes to the synthesis of new materials.

Smalley and co-workers[7,8] get the credit for the first attempt to synthesize boron-doped fullerene. They were able to detect several borafullerenes in the gas phase, $C_{60-n}B_n$ ($n = 1-6$), under mass-spectroscopic conditions after laser vaporization of graphite and boron nitride composites. Muhr et al.[9] developed a method for the preparation of macroscopic amounts of monosubstituted boron fullerenes ($C_{59}B$, $C_{69}B$, and higher homologues) utilizing doped graphite rods. Shinohara and co-workers[10] described the production of boron-doped carbon clusters via the laser vaporization cluster beam technique. Boron-doped heterofullerenes and onion-like cages have been synthesized[11,12] by in-situ irradiation of turbostatic B_xC_{1-x} ($x < 0.2$). Macroscopic quantities of B-doped fullerenes, such as $C_{60-n}B_n$ and $C_{70-n}B_n$ ($n = 1, 2$), were successfully synthesized[13] by the d.c. arc burning method of a graphite anode having a hole filled with tetraboron carbide.

Pradeep et al.[14] reported the preparation of nitrogen-doped fullerenes by contact arc vaporization of graphite in the presence of N_2 or NH_3. In this experiment, they observed even numbers of carbon substituted by nitrogen (such as $C_{59}N_2$, $C_{59}N_4$, $C_{59}N_6$, and $C_{70}N_2$) using mass spectroscopy. In the presence of pyrrole vapor instead of N_2 or NH_3, Glenis et al.[15] synthesized higher azafullerenes ($C_{60-2n}N_{2n}$, where $n = 1-23$) using the same technique. Hummelen et al.[16] found the effective formation of azafulleronium $C_{59}N^+$ in the gas phase during fast atom bombardment mass spectrometry of a cluster-opened *N*-methoxyethoxy methyl ketolactam. They applied this process in solution in the presence of strong acid and isolated the heterofullerene as its dimer $(C_{59}N)_2$. Recently, Reuther and Hirsch[17] summarized the synthetic methods, properties, and chemistry of $C_{59}N$.

Several theoretical investigations on borafullerene, namely $C_{59}B$,[18−21] $C_{58}B_2$,[22−26] $C_{60-x}B_x$ ($x = 2-8$),[27] and azafullerenes such as $C_{59}N$,[19−21,28] $C_{58}N_2$,[22−26] $C_{60-x}N_x$ ($x = 2-8$),[27] etc., have been devoted to understanding the effect of B and N substitution on structure, and electronic and chemical properties of fullerenes.

Besides trivalent B and N substitution, initiative has also been taken to substitute carbon of fullerene by divalent oxygen. Both the anion[29] and cation[30] of oxy-fullerene ($C_{59}O$) were generated in mass spectrometers in the gas phase. Synthesis of thiofullerene has been attempted by arc vaporization method and evidence of formation of $C_{60-2n}S_n$,$C_{60-3n}S_n$, and $C_{60-4n}S_n$ have been found.[31] Theoretical investigations on different oxidation states of $C_{59}O$[32−34] and $C_{59}S$[20,34] support both open and closed cage structures. The first silicon-doped carbon cluster has been detected by Kimura[10] using pulse-laser-vaporization of a silicon−carbon composite rod. The existence of sila-fullerenes with multiple Si substitution has been revealed by ion mobility[35] and mass spectroscopy.[36−39] Semiempirical and density functional theories have been used to study the structural arrangements, band gaps, nonlinear optical properties, and reactivity of mono- and di-Si-substituted fullerenes.[32,40−45]

Out of several heterofullerenes studied so far, overwhelming attention has been paid to hybrid B/C/N fullerenes because of

* Corresponding author. Tel: 1-435-797-7230. Fax: 1-435-797-3390. E-mail: tapaskar@cc.usu.edu.

10.1021/jp026547c CCC: $25.00
Published on Web 04/24/2003

their structural similarities. The other important factor lying behind such interest is that the BCN systems are isoelectronic with their parent carbon molecules. Several kinds of semiconductors can be expected from BCN materials. One is an intrinsic type of semiconductor, which can be converted to a p-type or an n-type extrinsic semiconductor by replacing C by B and N, respectively. Synthesis of BN-substituted fullerenes has been reported: by an electric arc burning technique using a graphite anode having a hole filled with boron nitride in inert atmosphere,[46] by high-temperature laser ablation of graphitic BCN,[47] by electron-beam irradiation of various precursors,[48,49] and by substitution reaction upon irradiation with a KrF excimer laser at room temperature.[50] Mass spectra and XPS confirmed the presence of B and N.

Several theoretical investigations[22,51−56] on mono-BN substitutionally doped fullerenes have been reported. These studies indicate that heteroatoms prefer to stay together. Location of B and N atoms in the cage structure has significant effects on electronic properties. Studies[57−60] on multiple (up to 3) BN substitution showed that these structures where BN units are connected to each other are most stable. It has been pointed out that stability of BN−fullerenes is enhanced when they contain the maximum number of B−N bonds.

Our previous theoretical investigations[61,62] on BN-substituted C_{60} fullerenes established the structural patterns of successive substitution of 1−24 carbon pairs by BN moieties. These studies also established certain rules of successive BN substitution in cage-like carbon materials, such as "hexagonal filling rule" and "N-site rule". It was found that heterofullerenes with less than 40% BN substitution have a lower band gap than does semiconducting C_{60}. We have also found that not only the number of heteroatoms may tune the properties of BN−fullerenes, but also their filling patterns. For example, completely BN-filled hexagons have larger gaps than do partially filled neighbors. Redox characteristics also strongly depend on the number of BN units and the filling pattern.

Similar to small BCN systems,[63,64] investigations on small AlCN systems are also in progress.[65,66] BelBruno[67] reported that the properties of AlN clusters are similar to those of the BN clusters, even though the aluminum atoms have a significantly larger atomic radius. Therefore, like BN, the wide range of engineering applications of AlN and the ability of fullerenes to form compound clusters with different compositions and size, provide hope of formation of a new class of materials of unique technological importance from $C_{60-n}(AlN)_n$ systems. Several studies on aluminum-coated fullerenes (Al_x-C_{60}) have been reported.[68−73] Although a reasonable amount of information is available on $C_{60-2x}(BN)_x$ systems, no investigations on Al-doped fullerene $C_{60-2x}(AlN)_x$ has been reported. Experimental evidence concerning substitutional doping of heteroatoms, including second-row elements such as Si and S, in a carbon cage-like network indicates that the possibility of Al and N doping may not be overlooked. Furthermore, doping of second-row heteroatoms causes significant changes in electrical and chemical properties of pure fullerene compared to their first-row analogues. Thus, an attempt to investigate AlN doping in fullerene seems worthwhile.

In the present investigation we carried out a systematic semiempirical and density functional calculation on $C_{60-2x}(AlN)_x$, where $x = 1-3$. The structural patterns, atomic arrangements, and heats of formation may provide useful information to experimentalists on the growth of AlN−fullerenes from pure carbon systems. Besides structural arrangements, we also intend to provide information on electronic and chemical properties of AlN-substituted fullerenes. Finally, the effect of successive substitution of AlN and BN in a C_{60}-ball is compared.

Method of Calculations

Since no theoretical or experimental investigation on AlN-substituted carbon fullerenes have been reported so far, no prior information is available on the AlN substitution patterns. Successive substitution patterns and atomic arrangements of BN−benzene systems[74−77] were found helpful to construct different isomers of BN−fullerenes. Thus, a preliminary investigation has been carried out on the much smaller AlN-substituted benzene molecule. Geometries of different mono- and di-AlN-substituted benzenes, $AlNC_4H_6$ and $(AlN)_2C_2H_6$, respectively, have been fully optimized using the density functional method, namely, B3LYP[78,79] with split-valence double-ζ quality basis functions (3-21G and 6-31G*). In addition to these higher level methods, semiempirical MNDO[80] and PM3[81] methods are employed to assess their reliability in determining the stability of different isomers. This will certainly provide us some guidance on the AlN substitution patterns in bigger carbon networks, and also on the reliability of MNDO and PM3 methods for Al−N−C systems.

Because of the size factor of AlN−fullerenes considered herein, full geometry optimization (without any symmetry constraints) were carried out using MNDO and PM3 methods. MNDO and PM3 have been used widely in previous investigations[57,59] on several heterofullerenes and found quite appropriate to determine structural and relative energies of different isomers of $C_{60-n}X_n$ (X = N, B, BN). In some cases where relative energies are within 1−3 kcal/mol, full geometry optimization has also been carried out using the B3LYP/3-21G method. Vibrational analyses at both MNDO and PM3 levels indicate that all isomers of 1−3 AlN−substituted C_{60} considered in the present investigation have no imaginary frequencies, indicating a true minimum. We explored several possible isomers in each case at the semiempirical level. Energetically favored species thus obtained were subsequently treated at B3LYP using 3-21G and B3LYP/3-21G* basis functions. It may be noted that the latter basis set contains polarization d-functions on Al atoms. Finally, the properties of the most stable isomers of each group were calculated using the B3LYP/6-31G* method.

It is worth mentioning that, in DFT methods, molecular orbitals are best termed Kohn−Sham (KS) orbitals. Very recently, it has been shown by Stowasser and Hoffmann[82] that the shape and symmetry of the KS orbitals are quite similar to those of the Hartree−Fock (HF) orbitals with which chemists are so familiar. The similarity between KS and HF orbitals has also been reported in several other articles.[83−85] These studies indicate that Koopmann's theorem, originally based on Hartree−Fock (HF) orbitals, can be used for KS orbitals to estimate ionization potential (IP) and electron affinity (EA). MNDO, PM3, and DFT calculations were performed using the Gaussian98, A.7, program.[86]

Results and Discussion

AlN-Substituted Benzene Molecules. As mentioned in the previous section, substitution of carbon pairs of benzene by AlN was investigated first. Relative energies of different mono- and di-AlN-substituted benzene molecules obtained using MNDO, PM3, B3LYP/3-21G, and B3LYP/6-31G* are summarized in Figure 1. Like its BN counterpart,[74−76] Al and N atoms prefer adjacent positions. Separation of these two atoms costs more than 20.0 kcal/mol. Multiple AlN substitution also follows patterns similar to those found in its BN counterpart.[75,77] In

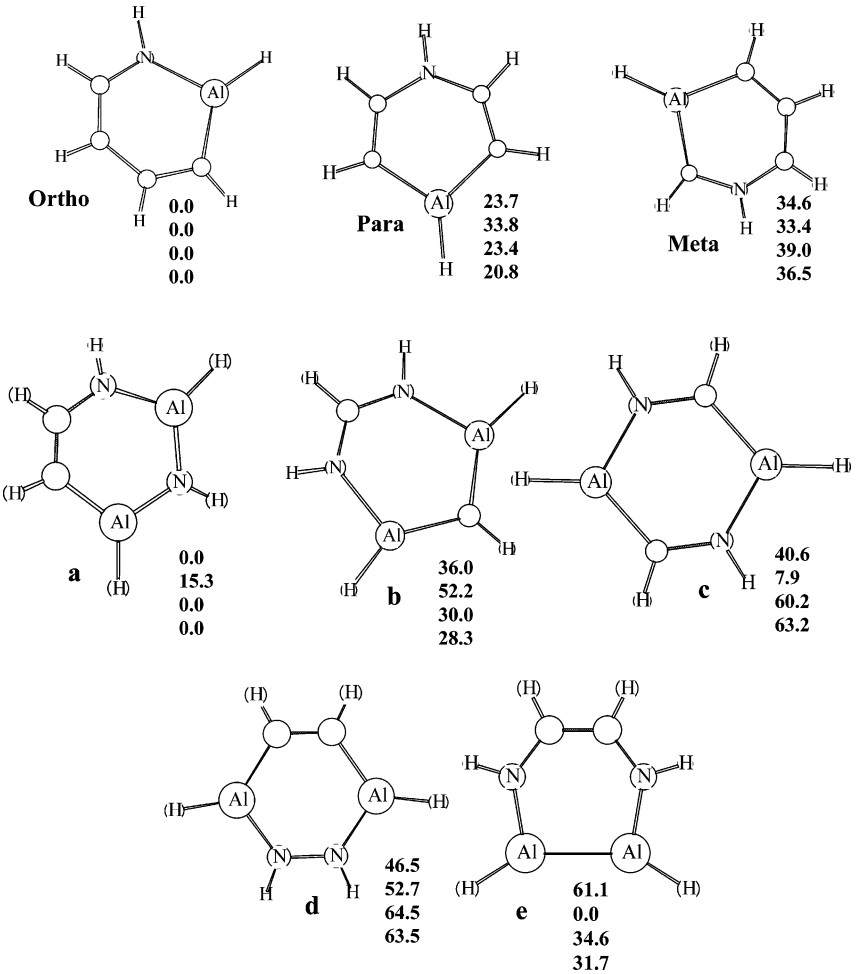

Figure 1. Isomers of mono (ortho, meta, and para) and di-AlN (**a**−**e**) substituted benzenes with relative energies (E_{rel} in kcal/mol). E_{rel} values are listed in the order of MNDO, PM3, B3LYP/3-21G, and B3LYP/6-31G*. Geometries are optimized at the same level of theory.

summary, stability is enhanced by keeping AlN units together as shown in **1a**, and AlAl and NN bonds are disfavored. Regarding various methods used, MNDO predictions are in line with DFT results. However, PM3 energies are not in the same order with other methods. For example, the most stable isomer **1a** of $(AlN)_2C_2H_6$ is higher in energy than isomer **1e** by 15 kcal/mol, while **1e** is predicted to be less stable than **1a** by more than 30.0 kcal/mol according to DFT methods and by about 60 kcal/mol according to MNDO. A close look at the optimized geometries of isomer **1e** indicates that in the PM3 structure, hydrogen atoms attached to aluminum approach one another close enough to approximate a hydrogen molecule, which is not the case for other the three methods. In case of mono-AlN substitution, both meta and para isomers are isoenergetic according to PM3, while the other three methods indicate an energy difference of 10−16 kcal/mol. Before any decisive conclusion on the reliability of the PM3 method for AlN−carbon systems, we would like to use this method for larger AlN−fullerene cases. It may be noted that the PM3 relative energies of mono- and di-AlN−benzenes obtained from the MOPAC 97[87] program also follow similar discrepancies.

AlN-Substituted C_{60}. A Schlegel diagram of C_{60} has been used in the present investigation to avoid 3-dimensional figures. In this diagram (Figure 2), not only are the positions of sixty carbon atoms shown, but also twelve pentagons and twenty hexagons are numbered as **P*n*** (n = 1 to 12) and **H*m*** (m = 1−20), respectively. For the description of different isomers, only those hexagons and pentagons of the Schlegel diagram where CC units are replaced by AlN moieties are shown in Figures 3, 4, and 5. It should be kept in mind that each pentagon is surrounded by five hexagons, and alternate pentagons and hexagons are around each hexagon of fullerenes. Relative energies (E_{rel}) of several isomers of AlN−fullerenes computed by MNDO, PM3, and B3LYP methods are summarized in

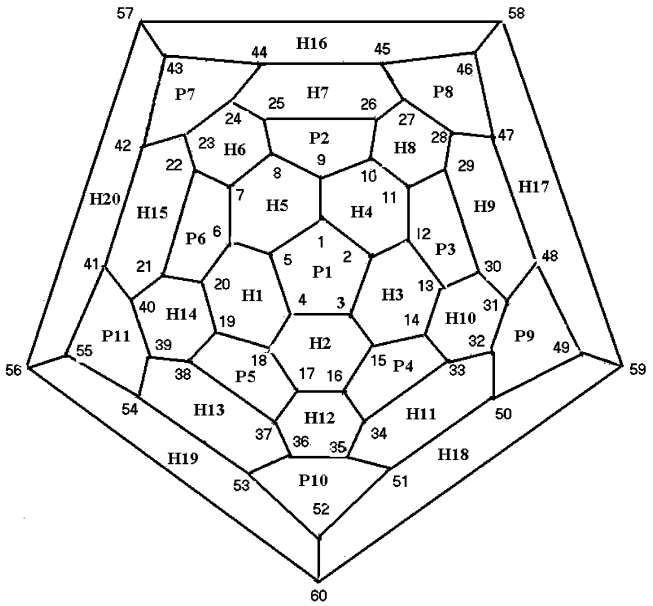

Figure 2. Schlegel diagram of C_{60}. **H** and **P** represent hexagon and pentagons, respectively.

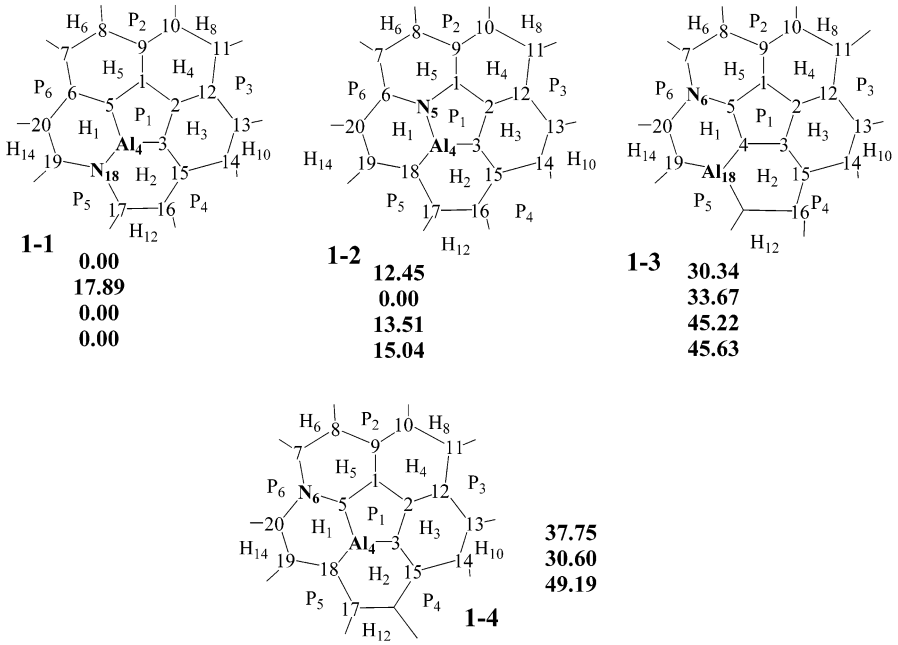

Figure 3. Isomers of 1-AlN−fullerenes with relative energies (E_{rel} in kcal/mol). E_{rel} values are listed in the order of MNDO, PM3, B3LYP/3-21G, and B3LYP/3-21G*. Only the relevant sections of the entire fullerene are shown. Same numbering scheme of the atoms and rings are maintained here and in Figures 4 and 5.

Figures 3, 4, and 5, along with their structural arrangements. Two integers have been used to identify those isomers; the first integer indicates the number of CC units replaced, and the second represents the isomer number. In all cases, the relative energy (E_{rel}) of the most stable isomer (ground state) of each group is assigned zero and less stable isomers are arranged with increasing order of E_{rel}. Throughout this study it is noticed that PM3 E_{rel} values do not fit well with those of other methods; therefore, PM3 energy values are ignored in arranging the sequences of the isomers. It may be worth mentioning that in this study we are not interested in the accuracy of the energy values or other properties, but rather in their trends. We will mainly focus on DFT results wherever calculated, otherwise MNDO.

A. Energetics. Although we studied several possible isomers of 1-AlN−fullerene $C_{58}AlN$, only those isomers within 40 kcal/mol (MNDO energies) of the most stable one are shown in Figure 3. Atomic arrangements considered in these isomers are shown along with relative energies. Although energy values strongly depend on different methods considered here, their trends are similar, except for the PM3 method. Such a discrepancy has already been noted in small aluminum−nitrogen-substituted benzene cases (Figure 1).

As in the case of 1-BN−fullerene $C_{58}BN$[22,51,52,55,59,61] and AlN−benzene, the heteroatoms prefer adjacent positions as shown in **1**−**1**. Separation of Al and N atoms, as in **1**−**3** and **1**−**4**, causes destabilization by more than 30 kcal/mol. Isomers with larger Al−N distance, i.e., with Al and N in different rings, are even less stable. It may be noted that energy ordering in **1**−**1**, **1**−**3**, and **1**−**4** are similar to that of ortho, para, and meta isomers, respectively, of AlN−benzenes (Figure 1). Another similarity with its BN counterpart is the position of the AlN bond, which also prefers hexagon−hexagon (**H**−**H**) junctions compared to hexagon−pentagon (**H**−**P**) junctions. The latter structural arrangement (**1**−**2**) is disfavored by more than 12 kcal/mol. However, PM3 predicts this isomer to be the most stable. Since this result does not tally with more accurate B3LYP methods, we bypass PM3 results. The inclusion of aluminum d-orbitals in the basis functions (as in 3-21G*) slightly lowers the E_{rel} values. The maximum change of 1.5 kcal/mol in relative energies of 1AlN−fullerenes is found in the **1**−**2** isomer.

Six isomers of 2AlN−fullerenes $C_{56}(AlN)_2$ (all those within 40 kcal/mol of the most stable one) obtained by replacing two CC units from the C_{60} ball are summarized in Figure 4. As found in the $C_{56}(BN)_2$ system, the most important factor for the stability of the present system is also the consecutiveness of AlN units, which creates additional AlN bonds connecting them. (It may be noted that those bonds are in general located at pentagon−hexagon junctions because of geometric arrangements of fullerenes). Similar to BN fullerenes[22,52,59,61] formation of extra AlN bonds might cause greater stability of the system. Separation of AlN units causes destabilization. As shown in **2**−**4**, **2**−**5**, and **2**−**6**, the stability of the isomers decreases as the AlN moieties are moved apart, even when they are located at **H**−**H** positions as in **2**−**6**. Once again, PM3 relative energies are inconsistent with MNDO.

Two AlN units are adjacent in the first three most stable isomers, namely, **2**−**1**, **2**−**2**, and **2**−**3** in this group (Figure 4). The second AlN unit is attached to the existing AlN unit of 1-AlN−fullerene (**1**−**1**). The difference among these isomers is the location of the incoming AlN unit. The most stable isomer of this group is **2**−**1**, which places the second AlN unit (N_5−Al_1) in $\mathbf{H_5}$−$\mathbf{P_1}$ junction. Interestingly this atomic arrangement differs from that of the most stable 2-BN−fullerene, where all four heteroatoms are located in one hexagon, similar to the arrangement in isomer **2**−**2**. The latter isomer is slightly unstable, and the energy difference is only within 1−2 kcal/mol (except the PM3 value). Since this small energy difference is obtained using MNDO optimized geometries (MNDO//MNDO, B3LYP/3-21G//MNDO, and B3LYP/3-21G*//MNDO methods), we further optimized the geometries of **2**−**1** and **2**−**2** at the B3LYP/3-21G level. The E_{rel} of **2**−**2** thus obtained is 3.1 kcal/mol, which reconfirms the stability of **2**−**1** over **2**−**2**.

The stability of **2**−**1** may be due to the large atomic size of the Al atom that prefers to situate itself in different consecutive rings to minimize structural damage of the hexagon and to maintain continuity of AlN units. A closer look at the geometries of **2**−**1** and **2**−**2** reveals that the sum of the six bond lengths of

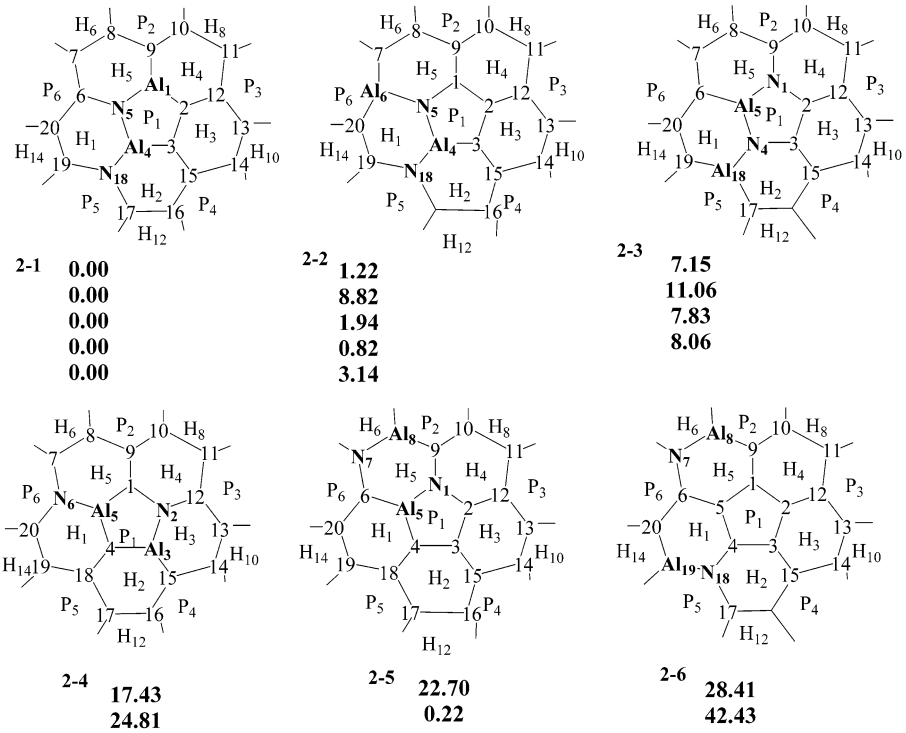

Figure 4. Isomers of 2-AlN−fullerenes with relative energies (E_{rel} in kcal/mol). E_{rel} values are listed in the order of MNDO, PM3, B3LYP/3-21G, B3LYP/3-21G*, and B3LYP/3-21G//B3LYP/3-21G.

hexagon $\mathbf{H_1}$ of **2**−**1** is 0.63 Å longer than that of C_{60}. This length difference is 1.36 Å in isomer **2**−**2**, a great deal of distortion when two Al atoms occupy the same hexagon. The atomic arrangement in **2**−**3**, which is about 7−8 kcal/mol less stable, is similar to that of the most stable isomer, except that Al and N positions are interchanged. Pentagon $\mathbf{P_1}$ of **2**−**3** contains two nitrogens, one aluminum, and two carbon atoms, while the most stable $\mathbf{P_1}$ of **2**−**1** consists of two Al, one N, and two C atoms. The NN distance in **2**−**3** is shorter by about 0.3 Å than the NN distance in the hexagon. Repulsion between two negatively charged (−0.7 at DFT/6-31G* method) N atoms placed closely in pentagon $\mathbf{P_1}$ might cause destabilization. It may be noted that nitrogen charges are about −0.5 at the same level of theory in BN−fullerenes. In fact, because of these negative charges NBN and NAlN angles are wider than BNB and AlNAl angles, respectively. Comparing these two isomers we find that extension from mono- to di-AlN substitution takes place via the Al atom of **1**−**1** to form **2**−**1**, while it is the nitrogen that is the attachment site in the case of **2**−**3**. Thus, the "N-site attachment rule"[61] of BN-substitution seems not valid for AlN−fullerene.

In the following figure, the structure and energy results of 3-AlN−fullerenes are summarized. Since separation of AlN moieties causes destabilization, no such arrangement has been consider for this group. The energy values (except PM3) indicate the preferred structure of 3-AlN−fullerene is **3**−**1**, which has one of the nitrogen atoms, i.e., N_5 attached to three aluminum atoms. This seems to be a ruling factor in AlN substitution patterns. If we consider that 3-AlN−fullerene is grown from its predecessor **2**−**1**, then the incoming third AlN unit does not prefer to form a zigzag chain as shown in **3**−**5**, rather heteroatoms join separately with existing N_5 and Al_1 atoms to form **3**−**1**.

An arrangement (**3**−**2**) where a hexagon is completely filled by AlN units is less stable by only 2 kcal/mol according to MNDO. PM3 supports the "hexagon filling rule"[61] as observed in BN−fullerenes. However, results from more reliable DFT methods are not in accordance with such findings. For further checks, geometries of **3**−**1** and **3**−**2** were optimized at the B3LYP/3-21G level. The relative energy of the latter isomer surpasses 20 kcal/mol, confirming **3**−**1** as the most stable isomer. Thus, PM3 once again fails to agree with MNDO and DFT. Interestingly, the PM3 method was able to predict the correct trend of energies for other heterofullerenes such as B−, N−, and BN−fullerenes.[25,26,57,59,88,89] The failure of the PM3 method may be a result of the parametrization of Al implemented in Gaussian98 and MOPAC97 programs.

Isomers where each nitrogen atom is surrounded by two aluminum atoms are less stable compared to those where all three surrounding atoms are Al. For example, the AlN arrangement of **3**−**3** has an environment similar to that of **3**−**1**, except nitrogen at position 5 is attached to two Al atoms. The same situation makes **3**−**5** less stable by 18 kcal/mol. However, an exactly opposite arrangement, where Al is attached to three N atoms as in **3**−**4**, causes destabilization because of close proximity of two negatively charged nitrogen atoms. This phenomenon, in addition to a larger number of less favorable AlN bonds in hexagon−pentagon junctions, makes **3**−**6** even more unstable by 4 kcal/mol.

In summary, AlN substitution patterns significantly differ from BN substitution patterns. The reason behind such differences may be due to the larger size of Al compared to that of B. The other crucial factor is the weak overlap of Al and N p-orbitals to form a π-network. An example of three π-MOs of benzene, 1-BN−benzene, and 1-AlN−benzene is shown in Figure 6. It is clear from these figures that π-interaction diminishes as we go from a BN to an AlN system. Delocalization of electrons (one of the dominating factors for the stability of cage structure) around AlN regions is significantly hindered by Al atoms. However, there are some similarities between BN− and AlN−fullerenes, e.g., heteroatoms do not prefer separation, and the filling starts at a hexagon−hexagon junction.

B. Changes in Electron Density. To compare the effects of BN and AlN substitution on the electron density of the parent

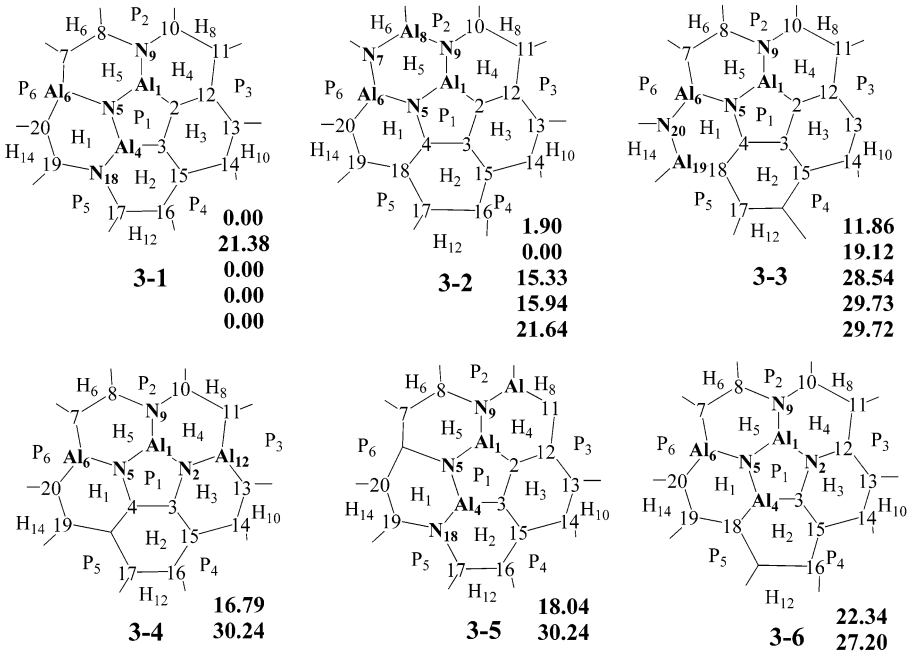

Figure 5. Isomers of 3-AlN−fullerenes with relative energies (E_{rel} in kcal/mol). E_{rel} values are listed in the order of MNDO, PM3, B3LYP/3-21G, B3LYP/3-21G*, and B3LYP/3-21G//B3LYP/3-21G.

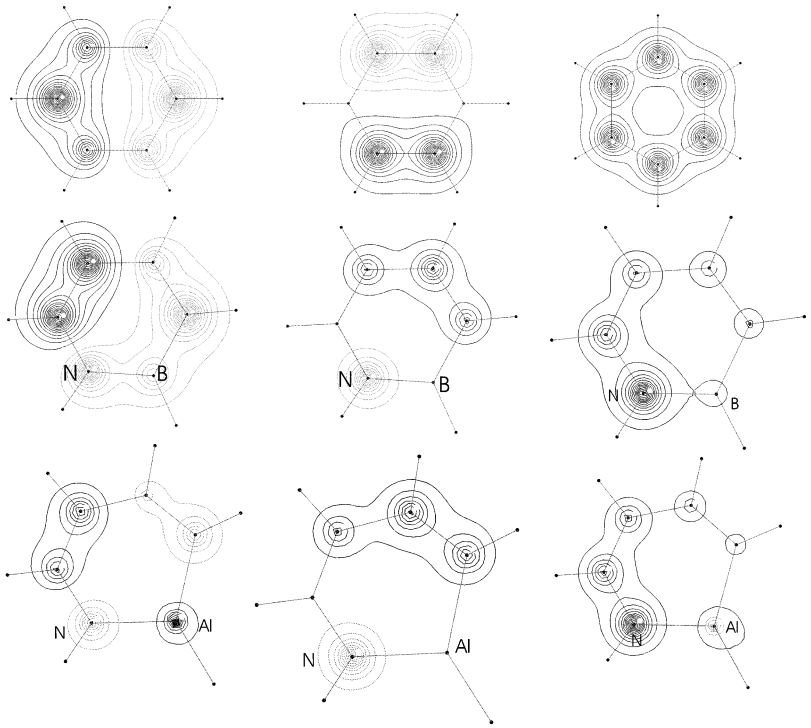

Figure 6. Three π-MOs of benzene, 1-BN−, and 1-AlN−benzene.

fullerene, two views (at different angles) of total electron density difference maps between 1-BN/AlN−fullerenes and C_{60} are illustrated in Figure 7. Such maps avoid any ambiguity of defining atomic charges, which are arbitrary by nature, and different schemes of partitioning electron density to one atom or another typically lead to discrepant charges. To avoid core electrons of Al atoms, semiempirical densities of only valence electrons are used. These maps were generated by comparing the MNDO density in 1-BN/AlN−fullerene, point by point in space, to the same quantity in the unsubstituted fullerene. Blue regions of these figures represent the accumulation of additional electron density as a result of heteroatom substitution; red regions indicate loss. AlN substitution clearly produces greater changes of electron density, compared to its BN counterpart. Nitrogen atoms gain some electron density, while loss is associated with electron deficient B and Al atoms. What is more important, the changes are more pronounced in the AlN case, because of the higher electronegativity difference between Al and N. For the same reason, carbon atoms attached to Al gain significant density compared to their attachment with boron atoms.

In the case of BN−fullerene, changes in density take place only in the close vicinity of B and N atoms; carbon atoms directly attached to a B(N) atom gain (lose) density. An

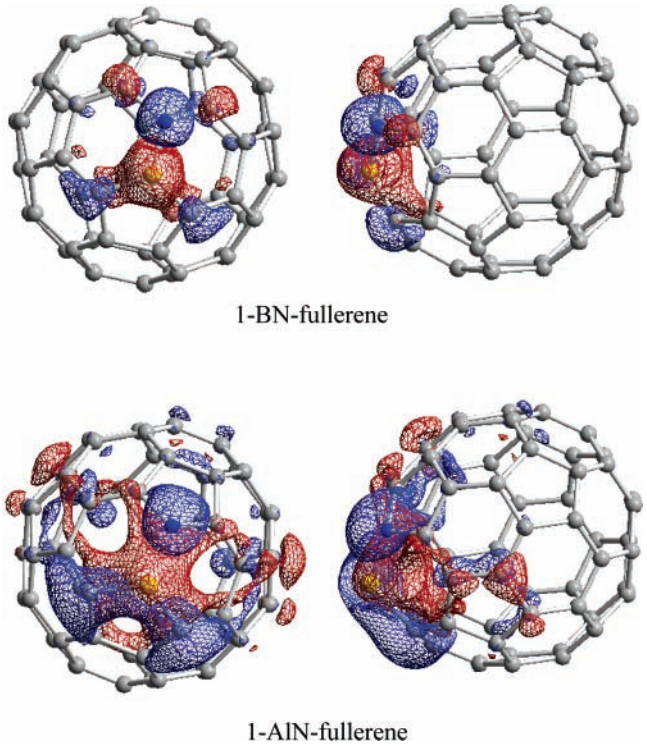

Figure 7. Maps of density differences between 1-BN/1-AlN−fullerenes and C_{60} fullerene. Two views at different angles are shown. The contour shown is 0.015 e/au^3. Blue regions denote gain, and red regions represent loss. Nitrogen and boron/aluminum atoms are shown in blue and yellow, respectively.

insignificant change in density is also observed on nearby carbon atoms. The situation is more complicated in the AlN case; blue/red regions are spread out over a wider space covering more than three carbon links. In a crude approximation (by counting the number of atoms with significant changes in densities), electron density of C_{60} is only 10% (four carbons attached to B and N plus the heteroatoms) distorted by one BN unit, while AlN substitution causes about 30% distortion. Thus, a larger number of carbon atoms of AlN−fullerenes gain (attached to Al atom) and lose (attached to N atoms) electron densities compared to that of BN−fullerene. These results indicate higher chemical (both electrophilic and nucleophilic) reactivities of AlN systems.

C. HOMO−LUMO Gap, Ionization Potentials, and Electron Affinities. HOMO−LUMO gaps (closely related to band gap) of most stable isomers of 1 to 3-AlN−fullerenes obtained from both semiempirical and density functional methods are plotted against the number of AlN units in Figure 8. For the sake of comparison, respective gaps[61] of BN−fullerenes have also been included in this figure. Although HOMO−LUMO gaps strongly depend on various methods, their trends are similar. Semiempirical MNDO and B3LYP/3-21G gaps are 2.33 and 1.04 times larger, respectively, than those of B3LYP/6-31G*. This ratio is almost independent of the number of AlN/BN units. It can be seen from Figure 8 that gaps of heterofullerenes strongly depend on the amount of substitution and have smaller values than in semiconducting C_{60}. As we move from BN to AlN, the gap further decreases. The first AlN substitution lowers the gap of C_{60} by 0.38 eV at DFT/6-31G* level. This change is about 0.23 eV in the case of 1-BN−fullerene. Significant lowering (0.53 eV) of band gap is noticed when AlN groups replace two CC pairs. In contrast, a slight increase (0.02 eV) is observed upon adding a second pair to 1-BN−fullerene. In both BN and AlN cases, replacement of a third CC pair causes a rise in gap

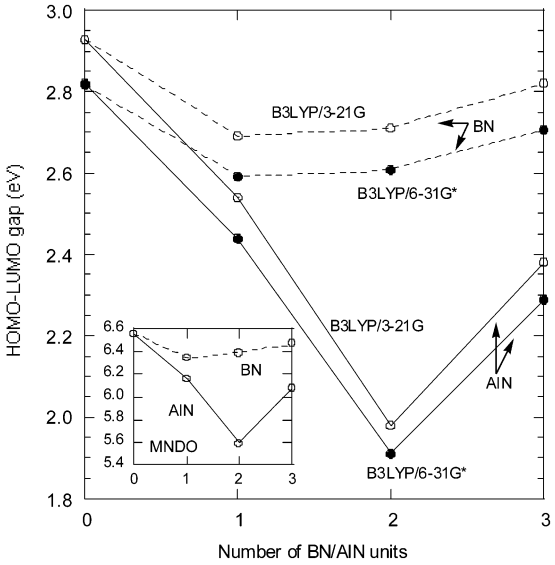

Figure 8. Variation of HOMO−LUMO gaps with the number of BN and AlN groups.

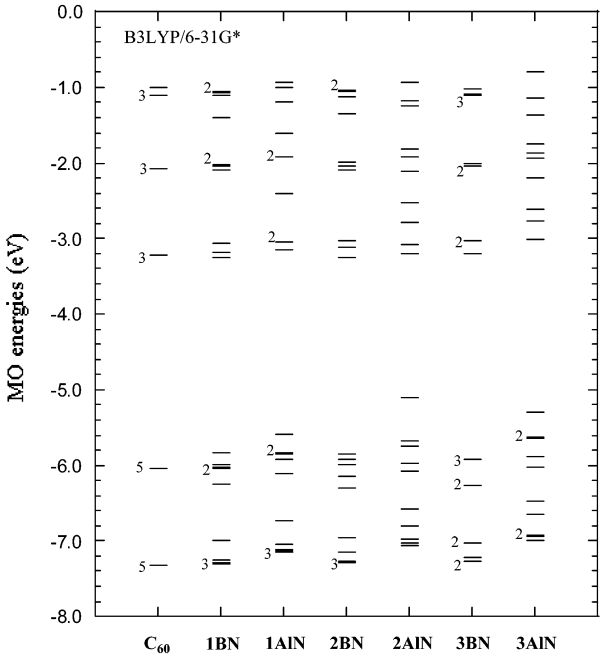

Figure 9. MO energies of C_{60}, BN−, and AlN−fullerenes. The number beside the MOs represents orbital degeneracy.

although they differ in atomic arrangements. This change is almost four times higher in 3-AlN−fullerene than in 3-BN−fullerene.

To analyze and compare the changes in the HOMO−LUMO gap and the effect of AlN and BN substitution on the energy levels of C_{60} near the Fermi level, 10 occupied and the same number of unoccupied orbital energies obtained from B3LYP/6-31G* methods are plotted in Figure 9 against the number of BN/AlN groups. (The number beside each level represents the orbital degeneracy.) In general, degeneracy of C_{60} MOs is lifted as CC pairs are replaced by either BN or AlN moieties. However, substituted fullerenes still retain some degenerate orbitals, except the 2AlN case. Compared to BN−fullerenes, the occupied MOs of AlN counterparts are more antibonding in nature, especially 2AlN−fullerene. No separate energy subband has been found for AlN groups in 2- and 3-AlN−fullerenes. This is also the case for unoccupied MOs,

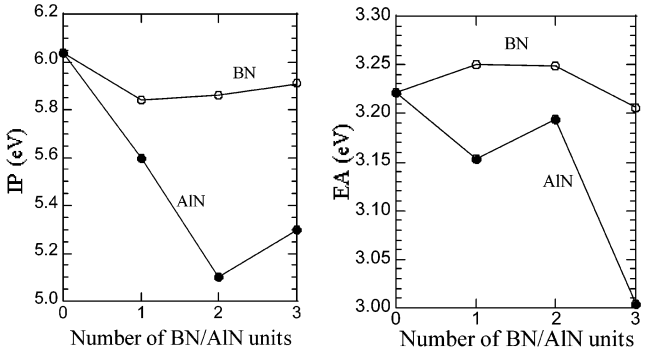

Figure 10. Variation of B3LYP/6-31G* ionization potential (IP in eV) and electron affinity (EA in eV) with the number of BN/AlN units.

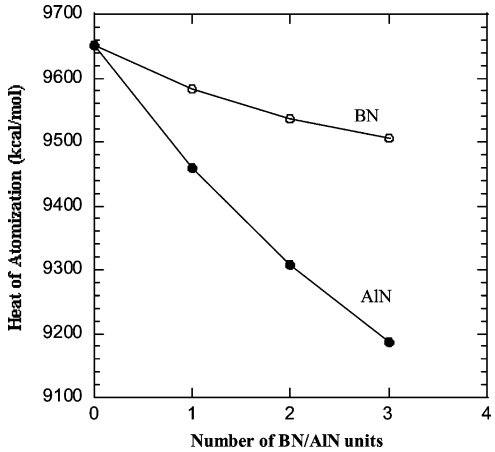

Figure 11. Variation of B3LYP/6-31G* heat of atomization with the number of BN/AlN units.

however, to a much lesser extent. The origin of the HOMO−LUMO gap of AlN systems is mainly due to the fluctuation of HOMOs.

DFT/6-31G*//MNDO ionization potentials (IP) and electron affinities (EA) of the most stable isomers of AlN and BN fullerenes are shown in Figure 10. The IP curve indicates that substituted fullerenes have somewhat smaller ionization potentials relative to C_{60} and the trend of IP curves is similar to that of the HOMO−LUMO gaps discussed earlier. From this figure it is clear the effect of AlN substitution on IP and EA is much more pronounced than that of BN counterparts. Mono substitution causes lowering in the ionization energies; a change of 0.20 and 0.44 eV in BN and AlN systems, respectively. Further replacement of CC units first causes a significant lowering (0.5 eV) of IP when aluminum is used and then a rise of 0.2 eV. So AlN fullerenes more easily lose an electron (oxidation) than their BN counterparts. Overall change in electron affinity is almost four times larger in AlN cages than in BN. Thus AlN fullerenes are easier to oxidize and reduce relative to BN cases. In short, redox characteristics of C_{60} may be tuned by substitutionally doping BN/AlN units.

Finally, we estimated DFT/6-31G* heats of atomization (H_{at}) of different substituted fullerenes considered herein by taking the energy difference of the fullerenes and their constituent atoms. Lower heat of atomization corresponds to higher energy and thus less stable and harder to synthesize. The H_{at} values are plotted against the number of BN/AlN units in Figure 11. The heat of atomization decreases in both BN and AlN cases, while for the latter case the change is much more sharp. These findings predict that, chemically and electronically, more active AlN−fullerenes will be harder to synthesize compared to BN systems.

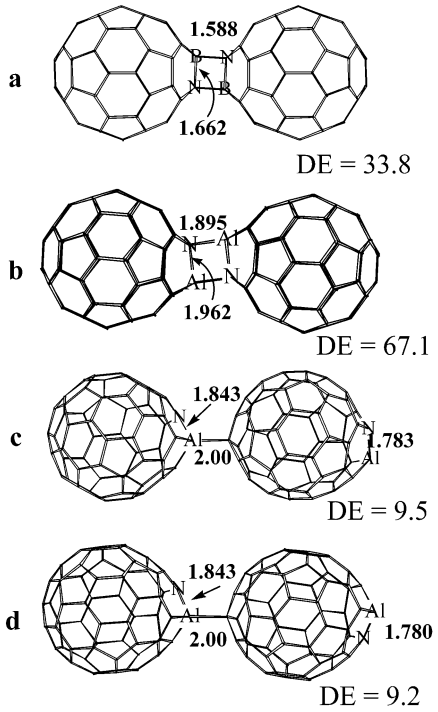

Figure 12. Isomers of $(C_{58}BN)_2$ (a) and $(C_{58}AlN)_2$ (b−d) with MNDO dimerization energy (kcal/mol) and bond distances (Å).

D. Dimer of $C_{58}BN$ and $C_{58}AlN$. The dimers of N-doped fullerenes, stable in solution[16] and in the solid state,[90,91] have been the subject of several experimental[92−99] and theoretical[28,100,101] investigations because of their chemical reactivity. The monomer units are connected via a single C−C bond formed by C atoms neighboring the N atoms of each monomer. Other studies[17] indicate a C−N bond connecting the two monomers. The dimer and trimer of $C_{58}BN$ have been reported by Gal'pern,[58] where several possible arrangements have been considered using MNDO theory. Thus, the presence of heteroatoms in doped fullerene makes it possible to polymerize. It is well know that aluminum compounds are stabilized by increasing coordination number from 3 to 4 or 6, forming dimers such as Al_2Cl_6.[102] The presence of both N and Al in the considered heterofullerenes leads us to study their dimer.

Several possible isomers of $(C_{58}BN)_2$ and $(C_{58}AlN)_2$ have been investigated using MNDO theory, and their structures along with relevant geometric parameters and dimerization energies (DE) are summarized in Figure 12. The isomers (**a** and **b**), where monomers are linked by four-membered B_2N_2 and Al_2N_2 cycles with alternation of the atoms, are the most stable for both BN− and AlN−fullerene dimers, respectively. The dimerization energy of $C_{60}AlN$ is almost double (67 kcal/mol) that of BN−fullerene. In both cases, the bridging A−N (A = B or Al) distance, connecting the monomers, is slightly shorter than the corresponding A−N distance of the monomers. Moreover, both these bonds are significantly elongated upon dimerization, because of the transformation of B/Al and N from sp^2 to sp^3.

In the head-to-tail isomer **c** of $C_{116}Al_2N_2$, two AlN−fullerenes are connected via an Al−C bond. This structure is stabilized by about 9.0 kcal/mol. No such structure with either a B−C or N−C bridging bonded dimer of $C_{116}B_2N_2$ has been found. In fact, in this dimer, the two units are separated from each other by about 5.5 Å, with negligible dimerization energy of 0.03 kcal/mol. Concerning its second-row counterpart, the other isomer **d**, where the position of Al and N atoms of one monomer is reversed, is isoenergetic with **c**. The bridging Al−C bond is about 0.2 Å longer than that of the other Al−C bond in AlN−

fullerene. The carbons of the second unit on the right in **c** and **d** are tera-coordinated. The four C−C bond lengths involving this sp^3 carbon are longer than any other C−C bonds and the <CCC angles fall in the range of 105 to 110°.

Conclusion

Successive substitution patterns of carbon pairs of fullerene by AlN moieties are studied using several methods, namely, MNDO, PM3, B3LYP/3-21G, B3LYP/3-21G*, and B3LYP/6-31G*. PM3 failed to agree with other methods considered herein regarding the trends of relative energies of the different isomers. Also, a comparison is made of electronic and chemical properties of AlN−fullerenes with its BN counterpart.

Like BN−fullerenes and BN−benzene, stability is enhanced by keeping not only Al and N atoms but also AlN units together. Single carbon pair replacement by AlN takes place at the hexagon−hexagon junction. However, a second substitution takes place in different fashion than BN systems and the "hexagon filling rule" of 3-BN−fullerene is disobeyed by 3-AlN−fullerene.

AlN−fullerenes, especially the 2-AlN−fullerene, have lower band gap than the corresponding BN-substituted fullerenes and by turn significantly lower gap than semiconducting C_{60}. Redox characteristics of fullerenes are enhanced significantly by AlN substitution. However, heat of atomization results indicate that AlN−fullerenes will be more difficult to synthesize than their BN analogues.

Several possible stable isomers of the AlN−fullerene dimer have been characterized. The most stable one is the structure where monomers are connected via an Al_2N_2 cycle. Similar structural arrangement is also common in BN−fullerene. The other possibility of an AlN dimer is via a Al−C bond; however, no such structure is found for $(C_{58}BN)_2$.

References and Notes

(1) Kroto, H. W.; Health, J. R.; O'Brien, S. C.; Curl, R. F.; Smalley, R. E. *Nature* **1985**, *318*, 162−165.

(2) Dresselhaus, M. S.; Dresselhaus, G.; Eklunf, P. C. *Science of Fullerenes and Carbon Nanotubes*; Academic Press: New York, 1996.

(3) *Fullerenes and fullerene nanostructures*; Kuzmany, H., Fink, J., Mehring, M., Roth, S., Eds.; World Scientific: Singapore, 1996.

(4) Harris, P. J. F. *Carbon Nanotubes and Related Structures, New Materials for the Twenty-first Century*; University Press: Cambridge, 1999.

(5) *Fullerenes and Related Structures*; Hirsch, A., Ed.; Springer: Berlin, 1999; Vol. 199.

(6) Cioslowski, J. *Electronic Structure Calculations on Fullerenes and their Derivatives*; Oxford University Press: New York, 1995.

(7) Guo, T.; Jin, C.; Smalley, R. E. *J. Phys. Chem.* **1991**, *95*, 4948−4950.

(8) Chai, Y.; Guo, T.; Jin, C.; Haufler, R. E.; Chibante, L. P. F.; Fure, J.; Wang, L.; Alford, J. M.; Smalley, R. E. *J. Phys. Chem.* **1991**, *95*, 7564−7568.

(9) Muhr, H. J.; Nesper, R.; Schnyder, B.; Koetz, R. *Chem. Phys. Lett.* **1996**, *249*, 399−405.

(10) Kimura, T.; Sugai, T.; Shinohara, H. *Chem. Phys. Lett.* **1996**, *256*, 269−273.

(11) Golberg, D.; Bando, Y.; Kurashima, K.; Sasaki, T. In *Mater. Res. Soc. Symp. Proc.* **1998**, *481*, 389−394.

(12) Golberg, D.; Bando, Y.; Kurashima, K.; Sasaki, T. *Carbon* **1999**, *37*, 293−299.

(13) Cao, B.; Zhou, X.; Shi, Z.; Gu, Z.; Xiao, H.; Wang, J. *Fullerene Sci. Technol.* **1998**, *6*, 639−648.

(14) Pradeep, T.; Vijayakrishnan, V.; Santra, A. K.; Rao, C. N. R. *J. Phys. Chem.* **1991**, *95*, 10564−10565.

(15) Glenis, S.; Cooke, S.; Chen, X.; Labes, M. M. *Chem. Mater.* **1994**, *6*.

(16) Hummelen, J. C.; Knight, B.; Pavlovich, J.; Gonzalez, R.; Wudl, F. *Science* **1995**, *269*, 1554−1556.

(17) Reuther, U.; Hirsch, A. *Carbon* **2000**, *38*, 1539−1549.

(18) Miyamoto, Y.; Hamada, N.; Oshiyama, A.; Saito, S. *Phys. Rev. B* **1992**, *46*, 1749−1753.

(19) Andreoni, W.; Gygi, F.; Parrinello, M. *Chem. Phys. Lett.* **1992**, *190*, 159−162.

(20) Kurita, N.; Kobayashi, K.; Kumahora, H.; Tago, K.; Ozawa, K. *Chem. Phys. Lett.* **1992**, *198*, 95−99.

(21) Chen, F.; Singh, D.; Jansen, S. A. *J. Phys. Chem.* **1993**, *97*, 10958−10963.

(22) Kurita, N.; Kobayashi, K.; Kumahora, H.; Tago, K. *Fullerene Sci. Technol.* **1993**, *1*, 319−328.

(23) Kurita, K.; Kobayashi, K.; Kumahora, H.; Tago, K. *Phys. Rev. B* **1993**, *48*, 4850−4854.

(24) Wang, S. H.; Chen, F.; Fann, Y. C.; Kashani, M.; Malaty, M.; Jansen, S. A. *J. Phys. Chem.* **1995**, *99*, 6801.

(25) Chen, Z.; Ma, K.; Pan, Y.; Zhao, X.; Tang, A.; Feng, J. *J. Chem. Soc., Faraday Trans.* **1998**, *94*, 2269−2276.

(26) Chen, Z.; Ma, K.; Pan, Y.; Zhao, X.; Tang, A. *Can. J. Chem.* **1999**, *77*, 291−298.

(27) Chen, Z.; Zhao, X.; Tang, A. *J. Phys. Chem. A* **1999**, *103*, 10961−10968.

(28) Andreoni, W.; Curioni, A.; Holczer, K.; Prassides, K.; Keshavarz-K, M.; Hummelen, J.-C.; Wudl, F. *J. Am. Chem. Soc.* **1996**, *118*, 11335−11336.

(29) Stry, J. J.; Garvey, J. F. *Chem. Phys. Lett.* **1995**, *243*, 199−204.

(30) Christian, J. F.; Wan, Z.; Anderson, S. L. *Chem. Phys. Lett.* **1992**, *199*, 373−378.

(31) Glenis, S.; Cooke, S.; Chen, X.; Labes, M. M. *Chem. Mater.* **1996**, *8*, 123−127.

(32) Lu, J.; Zhang, X.; Zhao, X. *Mod. Phy. Lett. B* **2000**, *14*, 23−29.

(33) Lu, J.; Zhang, S.; Zhang, X.; Zhao, X. *Solid State Commun.* **2001**, *118*, 247−250.

(34) Jiao, H.; Chen, Z.; Hirsch, A.; Thiel, W. *Phys. Chem. Chem. Phys.* **2002**, *4*, 4916−4920.

(35) Fye, J. L.; Jarrold, M. F. *J. Phys. Chem.* **1997**, *101*, 1836.

(36) Ray, C.; Pellarin, M.; Lerme, J. L.; Vialle, J. L.; Broyer, M.; Blase, X.; Melinon, P.; Keghelian, P.; Perez, A. *Phys. Rev. Lett.* **1998**, *80*, 5365−5368.

(37) Pellarin, M.; Ray, C.; Lerme, J.; Vialle, J. L.; Broyer, M.; Blase, X.; Keghelian, P.; Melinon, P.; Perez, A. *Eur. J. Phys.* **1999**, *9*, 49−54.

(38) Pellarin, M.; Ray, C.; Melinon, P.; Lerme, J.; Vialle, J. L.; Keghelian, P.; Perez, A.; Broyer, M. *Chem. Phys. Lett.* **1997**, *277*, 96−104.

(39) Billas, I. M. L.; Branz, W.; Malinowski, N.; Tast, F.; Heinebrodt, M.; Martin, T. P.; Massobrio, C.; Boero, M.; Parinello, M. *Nanostruct. Mater.* **1999**, *12*, 1071.

(40) Jacobs, S. J.; Rohlfing, C. M.; Cahill, P. A. In *Mater. Res. Soc. Symp. Proc.* **1995**, *359*, 363−368.

(41) Billas, I. M. L.; Massobrio, C.; Boero, M.; Parrinello, M.; Branz, W.; Tast, F.; Malinowski, N.; Heinebrodt, M.; Martin, T. P. *J. Chem. Phys.* **1999**, *111*, 6787−6796.

(42) Tenorio, F. J.; Robles, J. *Int. J. Quantum Chem.* **2000**, *80*, 220−226.

(43) Lu, J.; Luo, Y.; Huang, Y.; Zhang, X.; Zhao, X. *Solid State Commun.* **2001**, *118*, 309−312.

(44) Cheng, W. D.; Wu, D. S.; Zhang, H.; Chen, D. G.; Wang, H. X. *Phys. Rev. B* **2002**, *66*, 085422/1−085422/10.

(45) Fuks, I.; Kityk, I. V.; Kasperczyk, J.; Berdowski, J.; Schirmer, I. *Chem. Phys. Lett.* **2002**, *353*, 7−10.

(46) Piechota, J.; Byzsewski, P.; Jablonski, R.; Antonova, K. *Fullerene Sci. Technol.* **1996**, *4*, 491−507.

(47) Nakamura, T.; Ishikawa, K.; Yamamoto, K.; Ohana, T.; Fujiwara, S.; Koga, Y. *Phys. Chem. Chem. Phys.* **1999**, *1*, 2631−2633.

(48) Golberg, D.; Bando, Y.; Stephan, O.; Kurashima, K.; Sasaki, T.; Sato, T.; Goringe, C. In *International Conference on Solid-State Phase Transformations (JIMIC-3)*; Koiwa, M., Otsuka, K., Miyazaki, T., Eds.; Japan, 1999; pp 1301−1304.

(49) Golberg, D.; Bando, Y.; Stephan, O.; Bourgeois, L.; Kurashima, K.; Sasaki, T.; Sato, T.; Goringe, C. *J. Electron Microsc.* **1999**, *48*, 701−709.

(50) Nakamura, T.; Ishikawa, K.; Goto, A.; Ishihara, M.; Ohana, T.; Koga, Y. *Diamond Relat. Mater.* **2001**, *10*, 1228−1230.

(51) Liu, J.; Gu, B.; Han, R. *Solid State Commun.* **1992**, *84*, 807−10.

(52) Esfarjani, K.; Ohno, K.; Kawazoe, Y. *Phys. Rev. B* **1994**, *50*, 17830−17836.

(53) Esfarjani, K.; Ohno, K.; Kawazoe, Y. *Surf. Rev. Lett.* **1996**, *3*, 747−752.

(54) Esfarjani, K.; Ohno, K.; Kawazoe, Y.; Gu, B.-L. *Solid State Commun.* **1996**, *97*, 539−542.

(55) Piechota, J.; Byszewski, P. *Z. Phys. Chem.* **1997**, *200*, 147−155.

(56) Shkrabo, D. M.; Krasyukov, Y. N.; Mukhtarov, E. I.; Zhizhin, G. N. *J. Struct. Chem.* **1998**, *39*, 323−332.

(57) Chen, Z.; Ma, K.; Pan, Y.; Zhao, X.; Tang, A. *J. Mol. Struct. (THEOCHEM)* **1999**, *490*, 61−68.

(58) Gal'pern, E. G.; Stankevich, I. V.; Chistyakov, A. L.; Chernozatonskii, L. A. *Russ. Chem. Bull.* **1999**, *48*, 428−432.

(59) Chen, Z.; Ma, K.; Zhao, H.; Pan, Y.; Zhao, X.; Tang, A.; Feng, J. *J. Mol. Struct. (THEOCHEM)* **1999**, *466*, 127−135.
(60) Chen, Z.; Jiao, H.; Hirsch, A.; Thiel, W. *J. Org. Chem.* **2001**, *66*, 3380−3383.
(61) Pattanayak, J.; Kar, T.; Scheiner, S. *J. Phys. Chem A* **2001**, *105*, 8376−8384.
(62) Pattanayak, J.; Kar, T.; Scheiner, S. *J. Phys. Chem A* **2002**, *106*, 2970−2978.
(63) Kar, T.; Cuma, M.; Scheiner, S. *J. Phys. Chem. A* **1998**, *102*, 10134−10141.
(64) Kar, T.; Cuma, M.; Scheiner, S. *J. Mol. Struct. (THEOCHEM)* **2000**, *556*, 275−281.
(65) Gerasimov, I.; Yang, X.; Dagdigian, P. J. *J. Chem. Phys.* **1999**, *110*, 220−228.
(66) Meloni, G.; Gingerich, K. A. *J. Chem. Phys.* **1999**, *111*, 969−972.
(67) BelBruno, J. J. *Chem. Phys. Lett.* **1999**, *313*, 795−804.
(68) Hou, J. G.; Xiang, L.; Li, Y. Q.; Wang, H. Q. *Adv. Mater.* **1999**, *11*, 1124−1126.
(69) Hou, J. G.; Li, Y. Q.; Wang, Y.; Xu, W. T.; Zou, J.; Zhang, Y. H. *Phys. Status Solidi A* **1997**, *163*, 403−409.
(70) Zhang, X.-Y.; Hidalgo, R. Q.; Murphy, R. J.; Markiewicz, R. S.; Giessen, B. C. *Mater. Res. Soc. Symp. Proc. (Science and Technology of Fullerene Materials)* **1995**, *359*, 437−442.
(71) Li, Y.; Wang, Y.; Xu, W.; Hou, J. G.; Zhang, Y. H. *Physica C* **1997**, *282*−*287*, 737−738.
(72) Umemoto, M.; Liu, Z. G.; Masuyama, K.; Tsuchiya, K. *Mater. Sci. Forum* **1999**, *312*−*314*, 93−102.
(73) Slanina, Z.; Miyajima, C.; Zhao, X.; Uhlik, F.; Adamowicz, L.; Osawa, E. *Fullerene Sci. Technol.* **2000**, *8*, 385−402.
(74) Massey, S. T.; Zoellner, R. W. *Int. J. Quantum Chem.* **1991**, *39*, 787−804.
(75) Massey, S. T.; Zoellner, R. W. *Inorg. Chem.* **1991**, *30*, 1063−1066.
(76) Kranz, M.; Clark, T. *J. Org. Chem.* **1992**, *57*, 5492−5500.
(77) Kar, T.; Dalmore, D. E.; Scheiner, S. *J. Mol. Struct. (THEOCHEM)* **1997**, *392*, 65−74.
(78) Becke, A. D. *J. Chem. Phys.* **1992**, *96*, 2155−2160.
(79) Becke, A. D. *J. Chem. Phys.* **1993**, *98*, 5648−5652.
(80) Dewar, M. J. S.; Thiel, W. *J. Am. Chem. Soc.* **1977**, *99*, 4899−4907.
(81) Stewart, J. J. P. *J. Comput. Chem.* **1989**, *10*, 209−220.
(82) Stowasser, R.; Hoffmann, R. *J. Am. Chem. Soc.* **1999**, *121*, 3414−3420.
(83) Yang, W.; Mortier, W. J. *J. Am. Chem. Soc.* **1986**, *108*, 5708.
(84) Hoffmann, R. *J. Mol. Struct. (THEOCHEM)* **1998**, *424*, 1−6.
(85) Kar, T.; Angyan, J. G.; Sannigrahi, A. B. *J. Phys. Chem.* **2000**, *104*, 9953−9963.
(86) Frisch, M. J.; Trucks, H. B.; Schlegel, G. W.; Scuseria, G. E.; Robb, M. A.; Cheeseman, J. R.; Zakrzewski, V. G.; Montgomery, J. A., Jr.; Stratmann, R. E.; Burant, J. C.; Dapprich, S.; Millam, J. M.; Daniels, A. D.; Kudin, K. N.; Strain, M. C.; Farkas, O.; Tomasi, J.; Barone, V.; Cossi, M.; Cammi, R.; Mennucci, B.; Pomelli, C.; Adamo, C.; Clifford, S.; Ochterski, J.; Petersson, G. A.; Ayala, P. Y.; Cui, Q.; Morokuma, K.; Malick, D. K.; Rabuck, A. D.; Raghavachari, K.; Foresman, J. B.; Cioslowski, J.; Ortiz, J. V.; Baboul, A. G.; Stefanov, B. B.; Liu, G.; Liashenko, A.; Piskorz, P.; Komaromi, I.; Gomperts, R.; Martin, R. L.; Fox, D. J.; Keith, T.; Al-Laham, M. A.; Peng, C. Y.; Nanayakkara, A.; Gonzalez, C.; Challacombe, M.; Gill, P. M. W.; Johnson, B.; Chen, W.; Wong, M. W.; Andres, J. L.; Gonzalez, C.; Head-Gordon, M.; Replogle, E. S.; Pople, J. A. *Gaussian 98*; Gaussian, Inc.: Pittsburgh, PA, 1998.
(87) Stewart, J. J. J. *Chem3D*, CambridgeSoft Corp., Cambridge, MA. 1997.
(88) Chen, Z.; Reuther, U.; Hirsch, A.; Thiel, W. *J. Phys. Chem. A* **2001**, *105*, 8105−8110.
(89) Chen, Z.; Ma, K.; Chen, L.; Zhao, H.; Pan, Y.; X., Z.; Tang, A.; Feng, J. *J. Mol. Struct. (THEOCHEM)* **1998**, *452*, 219−225.
(90) Brown, C. M.; Beer, E.; Bellavia, C.; Cristofolini, L.; Gonzalez, R.; Hanfland, M.; Haeusermann, D.; Keshavarz-K, M.; Kordatos, K.; et al. *J. Am. Chem. Soc.* **1996**, *118*, 8715−8716.
(91) Brown, C. M.; Cristofolini, L.; Kordatos, K.; Prassides, K.; Bellavia, C.; Gonzalez, R.; Keshavarz-K, M.; Wudl, F.; Cheetham, A. K.; et al. *Chem. Mater.* **1996**, *8*, 2548−2550.
(92) Bellavia-Lund, C.; Gonzalez, R.; Hummelen, J. C.; Hicks, R. G.; Sastre, A.; Wudl, F. *J. Am. Chem. Soc.* **1997**, *119*, 2946−2947.
(93) Butcher, M. J.; Jones, F. H.; Beton, P. H.; Moriarty, P.; Prassides, K.; Tagmatarchis, N. In *AIP Conference Proceedings* 1999; Vol. 486, pp 165−169.
(94) Rachdi, F.; Hajji, L.; Dollt, H.; Ribet, M.; Yildirim, T.; Fischer, J. E.; Goze, C.; Mehring, M.; Hirsch, A.; Nuber, B. *Carbon* **1998**, *36*, 607−611.
(95) Haffner, S.; Pichler, T.; Knupfer, M.; Umlauf, B.; Friedlein, R.; Golden, M. S.; Fink, J.; Keshavarz-K, M.; Bellavia-Lund, C.; Sastre, A.; Hummelen, J. C.; Wudl, F. *Eur. Phys. J. B* **1998**, *1*, 11−17.
(96) Auerhammer, J. M.; Kim, T.; Knupfer, M.; Golden, M. S.; Fink, J.; Tagmatarchis, N.; Prassides, K. In *AIP Conference Proceedings* 2000; Vol. 544, pp 103−106.
(97) Wan, X.-G.; Dong, J.-M.; Xing, D. Y. *Commun. Theor. Phys.* **1999**, *32*, 515−520.
(98) Krause, M.; Baes-Fischlmair, S.; Pfeiffer, R.; Plank, W.; Pichler, T.; Kuzmany, H.; Tagmatarchis, N.; Prassides, K. *J. Phys. Chem. B* **2001**, *105*, 11964−11969.
(99) Auerhammer, J. M.; Kim, T.; Knupfer, M.; Golden, M. S.; Fink, J.; Tagmatarchis, N.; Prassides, K. *Solid State Commun.* **2001**, *117*, 697−701.
(100) Buehl, M.; Curioni, A.; Andreoni, W. *Chem. Phys. Lett.* **1997**, *274*, 231−234.
(101) Lee, K. H.; Park, S. S.; Suh, Y.; Yamabe, T.; Osawa, E.; Luethi, H. P.; Gutta, P.; Lee, C. *J. Am. Chem. Soc.* **2001**, *123*, 11085−11086.
(102) Cotton, A. F.; Wilkinson, G. *Advanced Inorganic Chemistry*, 5th ed.; John Wiley & Sons: New York, 1988.